HHS Public Access

Author manuscript

Genes Immun. Author manuscript; available in PMC 2014 March 01.

Published in final edited form as:

Genes Immun. 2013 September ; 14(6): 380–386. doi:10.1038/gene.2013.32.

Genetic control of murine invariant natural killer T-cells maps to multiple type 1 diabetes regions

Shirng-Wern Tsaih[1,*], **Shamim Khaja**[1,2,*], **Ashley E. Ciecko**[1,2], **Erin MacKinney**[1,2], and **Yi-Guang Chen**[1,2]

[1]Human and Molecular Genetics Center, Medical College of Wisconsin, Milwaukee, WI 53226

[2]Max McGee National Research Center for Juvenile Diabetes, Department of Pediatrics at the Medical College of Wisconsin, Milwaukee, WI 53226

Abstract

Reduced frequency of invariant natural killer T (iNKT)-cells has been indicated as a contributing factor to type 1 diabetes (T1D) development in NOD mice. To further understand the genetic basis of the defect, we generated (NOD X ICR)F2 mice to map genes that control iNKT-cell development. We determined frequencies of thymic and splenic iNKT-cells as well as the ratio of CD4-positive and -negative subsets in the spleens of 209 F2 males. Quantitative trait loci (QTL) analysis revealed 5 loci that exceed the significant threshold for the frequency of thymic and/or splenic iNKT-cells on Chromosomes (Chr) 1, 5, 6, 12, and 17. Three significant loci on Chr 1, 4, and 5 were found for the ratio of CD4-positive and -negative splenic iNKT-cells. Comparisons to previously known mouse T1D susceptibility (*Idd*) loci revealed two significant QTL peak locations respectively mapped to *Idd* regions on Chr 4 and 6. The peak marker location of the significant Chr 12 iNKT QTL maps to within 0.5Mb of a syntenic human T1D locus. Collectively, our results reveal several novel loci controlling iNKT-cell development and provide additional information for future T1D genetic studies.

Keywords

iNKT-cell; NOD mouse; Autoimmunity; Linkage analysis

Introduction

CD1d-restricted invariant natural killer T (iNKT)-cells are a unique population with diverse immunoregulatory functions [1]. Distinct from conventional CD4 and CD8 T-cells, iNKT-cells are selected by CD1d-expressing CD4/CD8 double positive (DP) thymocytes and

Address correspondence to: Dr. Yi-Guang Chen, Assistant Professor, Medical College of Wisconsin, Department of Pediatrics, Milwaukee, WI 53226, USA, Phone-414-955-7583, FAX-414-955-6516, yichen@mcw.edu.

*Contributed equally to work

Conflict of interest

The authors have no financial conflicts of interest.

Supplementary information is available at the Genes and Immunity's website

thereafter in mice develop into $CD4^+$ or CD4/CD8 double negative (DN) subsets [2, 3]. iNKT-cells can promote immune responses against tumors and infectious organisms, but they are also paradoxically capable of suppressing autoimmunity [4]. The frequencies of iNKT-cell vary significantly in humans [5–9]. Although the extent to which environmental factors may alter the frequency of iNKT-cells in humans is not known, it appears that this phenotype is largely genetically controlled [9]. Studies using a limited set of inbred mouse strains showed a high degree of variation in iNKT-cell frequencies in the liver [10]. Recently, we extended the previous studies using a large panel of classical and wild-derived inbred mouse strains. Consistent with the observation in humans, we also demonstrated a substantial strain-dependent variation in the frequencies of thymic and splenic iNKT cells, and those circulating in the blood [11]. Taken together, these results indicate that the development of iNKT-cells is a complex trait controlled by multiple genetic variants in both humans and mice.

Defects in iNKT-cells have been linked to several diseases, including autoimmune type 1 diabetes (T1D) [12]. In the NOD mouse model of T1D, disease development partly results from the numerical and functional defects in iNKT-cells characterizing this strain [13]. This conclusion is based on the findings that NOD mice were protected from T1D by administration of the iNKT-cell super-agonist α-galactosylceramide (α-GalCer) [14–17]. In addition, it has been reported that CD1d-deficient NOD mice lacking iNKT-cells developed accelerated T1D [17, 18]. Moreover, increasing iNKT-cell numbers by adoptive transfer prevented T1D development in NOD mice [19, 20]. Multiple T1D susceptibility (*Idd*) loci, including *Idd9.1* and *Idd13*, have been associated with an altered iNKT-cell compartment and likely contribute to disease development in NOD mice by limiting the generation or function of these immune regulators [21–25]. Previous studies using a backcross approach from C57BL/6 (B6) to NOD.*Nkrp1*^{b} mice identified two loci respectively on Chromosomes (Chr) 1 and 2 significantly linked to the frequency of thymic iNKT-cells [26]. Both loci (*Nkt1* and *Nkt2*) were subsequently confirmed by congenic analysis, and *Slamf1* and *Slamf6* within the *Nkt1* locus have also been shown to regulate iNKT-cell development [23, 27–29]. The B6-derived *Nkt2* locus has also been shown to suppress T1D in NOD mice [23].

Unlike the mouse studies, the potential role of iNKT-cells in human T1D remains controversial [12]. Early studies indicated that frequencies of iNKT-cells were reduced in T1D patients and functionally they were altered with an impaired ability to produce Th2 cytokines [30, 31]. However, these observations were later challenged by others as the numerical and functional differences between iNKT-cells in human T1D patients and control subjects were not consistently reported [9, 32]. It has also been reported that while no differences were found in the frequencies of total iNKT-cells, the proportions of the $CD4^+$ subset were significantly reduced in humans with or at high risk for T1D [6, 7]. These results are consistent with the idea that different iNKT-cell subpopulations have distinct functions and those expressing CD4 preferentially promote tolerance and conversely the DN subset contributes to anti-tumor activity and autoimmune pathogenicity [33–35]. It has also been shown that $CD4^+$ iNKT cells suppressed T1D whereas the DN subset promoted diabetes development in NOD mice [36, 37].

One approach to further determine if iNKT-cells modulate the development of T1D in humans is to ask if disease susceptibility genes or the pathways in which they participate are also involved in controlling the frequency and/or functional activity of this immunoregulatory population. We reasoned that this approach can be facilitated by information gained from the NOD model. The goal of the current study was to identify additional genetic regions that contribute to reduced iNKT-cells in the NOD strain and to determine if they overlap with previously known T1D regions in mice and humans. We carried out quantitative trait loci (QTL) analysis in a (NOD X ICR/HaJ)F2 cross. While sharing the same $H2^{g7}$ haplotype with NOD mice, the ICR/HaJ strain is completely resistant to T1D (Chen et al., unpublished results). We took advantage that both NOD and ICR/HaJ are related Swiss-derived strains originating from an Ha/ICR outbred stock [38], but differ significantly in their iNKT-cell frequencies [11]. Therefore, genetic regions that are identical by decent can be excluded in future analyses. We report here the identification of several novel and previously reported QTL that control the frequency of thymic and/or splenic iNKT-cells as well as the ratio of splenic CD4 and DN subsets. Interestingly, some of these QTL overlap with previously identified mouse *Idd* and syntenic human T1D regions.

Results

Analysis of iNKT-cells in NOD, ICR, and (NOD x ICR)F1 mice

CD1d tetramers in combination with anti-TCR_β were used to identify iNKT-cells in the thymus and the spleen (Fig. 1A). As previously reported [11], ICR mice had significantly higher percentages of iNKT-cells among total cells in both the thymus and the spleen than those in the NOD strain (Fig. 1A–1C). This observation remained the same when the frequencies of thymic and splenic iNKT-cells were normalized respectively to total TCR^{high} and TCR^+ cells (Fig. 1E and 1F; see supplementary Figure 1 for the gating strategy). (NOD x ICR)F1 mice displayed an intermediate phenotype in both the thymus and the spleen (Fig. 1). As $CD4^+$ and DN iNKT-cells are functionally distinct, we also determined the ratio of these two subsets in the spleen. NOD mice had proportionally reduced splenic $CD4^+$ iNKT-cells compared to either ICR or (NOD x ICR)F1 mice (Fig. 1G).

Main effect single-locus genome scans for QTL associated with thymic and splenic iNKT-cells

Analyses of 209 (NOD x ICR)F2 mice revealed a wide range of distribution for the frequency of both thymic and splenic iNKT-cells (Fig. 1B and 1C). The single locus genome scan for main effects identified two significant loci on Chr 12 and 17 regulating the frequency of thymic iNKT-cells (Fig. 2A and summarized in Table 1). Two significant loci on Chr 5 and 17, were identified for the frequency of splenic iNKT-cells (Fig. 2B and summarized in Table 2). Several suggestive QTL were also found on Chr 1, 4, 6, 11, and 13 (summarized in supplementary Tables 1 and 2). The F2 mice also showed variation in the percentages of total thymic TCR^{high} and splenic TCR^+ cells (data not shown). iNKT-cells and conventional T-cells originate from the same precursors. It is possible that the identified QTL regulated the overall frequency of T-cell progenitors. Therefore, we also conducted genome wide scans for the proportion of iNKT-cells among total TCR^{high} (thymus) and TCR^+ (spleen) cells. The results of these analyses are shown in Figures 2C and 2D and

summarized in Tables 1 and 2. All thymic and splenic iNKT-cell frequency QTL remain significant after adjusting respectively for total TCR^{high} and TCR^{+} cells. These results indicated that the major effects of the identified QTL functioned through regulating development of iNKT-cells rather than total T-cells. Two suggestive QTL for the frequency of splenic iNKT-cells respectively on Chr 1 and 6 became significant after adjusting for TCR^{+} cells (Table 2 and supplementary Table 2). Previous studies have shown that peripheral $CD4^{+}$ and DN iNKT-cells are functionally distinct [33–37]. Therefore, we also analyzed these two broad subsets of iNKT-cells based on CD4 expression in the spleens of the F2 mice. The genome wide scan identified three significant loci on Chr 1, 4, and 5 for the ratio of CD4/DN iNKT-cells (Fig. 2E and summarized in Table 2). A suggestive QTL was found on Chr 11 (supplementary Table 2).

Comparing thymic and splenic QTL revealed distinct loci (Tables 1 and 2, and supplementary Tables 1 and 2). This suggested that thymus-independent factors existed to modulate the accumulation of iNKT-cells in the spleen. To test this possibility, we performed QTL analysis on the frequency of splenic iNKT-cells with the thymic counterpart as a covariant (see Materials and Methods). After conditioning on the frequency of thymic iNKT-cells, only the Chr 5 QTL remained significant for the iNKT-cell frequency of total splenocytes or of splenic TCR^{+} cells (Fig. 3). The results indicated that accumulation of splenic iNKT-cells was largely dependent on the thymic output, but an ICR-derived gene(s) on Chr 5 preferentially enhanced the frequency of these immunoregulators in the spleen.

Pair-wise genome scans and multiple regression analysis for QTL associated with thymic and splenic iNKT-cells

To reveal interactive QTL associated with iNKT-cells, we performed a search to examine all possible locus pairs for additive and epistatic effects on the phenotype values. In this analysis it is also possible to identify significant main effects that were missed in the single-locus genome scans. Following pair-wise scans, we constructed a multiple QTL model to describe the simultaneous effects of all main and interacting QTL on the traits. QTLs may be removed if they fail to achieve a significant level after the effects of other QTL have been taken into account. The results are summarized in Tables 3 and 4. All significant and suggestive thymic and splenic iNKT-cell QTL were retained in the multiple regression model. Several new QTL were found on Chr 5, 13, and 15 for the thymic iNKT-cell traits. In this analysis, we also identified three new splenic iNKT-cell QTL on Chr 5, 8, and 16. These new loci identified in the pair-wise scans had relatively smaller effects compared to the significant QTL revealed in the single-locus genome scans. We did not find any significant epistatic interaction in all iNKT-cell traits.

Co-localization of iNKT-cell QTL with mouse and human T1D regions

We next determined if any of the iNKT-cell QTL identified in the current study was co-localized with previously known mouse and syntenic human T1D regions. This was done by comparing iNKT-cell QTL regions with the curated mouse *Idd* and the syntenic human T1D loci at T1DBase (http://www.t1dbase.org). For the purpose of this comparison, we only report a co-localization when a QTL peak marker location is within a defined mouse *Idd* or less than 0.5Mb apart from a syntenic human T1D region. This analysis revealed several

iNKT-cell QTL to be co-localized with previously identified mouse *Idd* regions, including *Idd9.2* on Chr 4, *Idd15* on Chr 5, *Idd6* complex on Chr 6, and *Idd14* on Chr 13 (summarized in Tables 1–4). Interestingly, the peak marker location of the Chr 12 iNKT-cell QTL mapped to within 0.5Mb of a syntenic human T1D locus on Chr 14 [39]. The syntenic region of the human T1D locus on Chr 14 (101.29–101.33Mb) is from 110.78Mb to110.81Mb on mouse Chr 12, about 0.25Mb apart from the QTL peak marker located at 110.53Mb (Figure 4).

Discussion

We previously showed that NOD mice had significantly reduced frequency of iNKT-cells compared to most other mouse strains [11]. In contrast, ICR mice were at the higher end of the spectrum compared to other strains [11]. In the current study, we generated a cohort of (NOD X ICR)F2 male mice to map genetic regions that control the frequency and subset of iNKT-cells in the thymus and the spleen. Through our genome scans, we identified significant QTL located on 6 chromosomes that modulate the frequency of thymic and splenic iNKT-cells as well as the ratio of splenic CD4/DN subsets. Although not too surprising, some NOD alleles were found to increase the frequencies of thymic and splenic iNKT-cells. Most likely these iNKT-cell promoting variants are masked in NOD mice by other genetic defects that significantly impair the development and accumulation of these immunoregulators. We also identified several suggestive QTL for the development and accumulation of iNKT-cells. Although we cannot rule out the possibility that the suggestive QTL are false positive, however, previous studies have shown that a suggestive locus could be concealed by other major QTL. For example, a Chr 11 region was not found significant in a cross between NOD and NOR strains for diabetes development, but congenic analysis revealed a role of the NOR-derived *Idd4* to suppress T1D [40, 41]. Validation of the suggestive QTL will require generation of congenic strains.

Through analyses of knockout mice, several genes have been identified that mostly intrinsically and to a less extent extrinsically control different stages of iNKT-cell development [42, 43]. Therefore, it is possible that the genetic loci identified here can function through iNKT-cell intrinsic mechanisms. It is also possible that iNKT-cell extrinsic factors underlie their defects in NOD mice. In our preliminary analysis, we found that NOD and ICR CD4/CD8 DP thymocytes expressed different levels of CD1d molecules, implying a role of iNKT-cell extrinsic factor dependent regulation of their differential development in these two strains. Further studies are required to determine how the genetic loci identified here regulate iNKT-cell development.

Previous linkage studies and congenic analyses reported by others and us identified genetic loci on Chr 1, 2, and 4 that reduce iNKT-cell development in NOD mice [22–26, 28, 44]. Compared to the previous linkage studies, the splenic QTL on Chr 1 (peaks at 172.96Mb) identified here overlaps with the *Nkt1* locus that contains *Slamf1* and *Slamf6* genes known to regulate iNKT-cell development [27, 29]. However, we did not detect a QTL overlapping the *Nkt2* region on Chr 2 or the *Idd9.1* region on Chr 4 reported to control iNKT-cell development. This indicates that the *Nkt2* and *Idd9.1* region genes responsible for the control of iNKT-cell development are not polymorphic between NOD and ICR strains. In

this study, we also identified several novel iNKT-cell modulating loci including a major QTL peak on Chr17 (distal to the *H2* locus) that regulates thymic and splenic iNKT-cell freqiencies. Further analysis of this region will require generation of a new congenic strain. CD4 and DN subsets of iNKT-cells are functionally distinct. Therefore, we also carried out QTL analysis to identify genetic loci that regulate the ratio of CD4 and DN iNKT-cell subsets. To our knowledge, this is the first report of such analysis to determine the genetic control of iNKT-cell subset differentiation. Interestingly, the *Nkt1* locus on Chr 1 also regulated the ratio of splenic CD4 and DN iNKT-cells. A QTL within the *Idd9.2* locus on Chr 4 was also found to regulate the ratio of splenic CD4 and DN iNKT-cells, suggesting a possible mechanism of *Idd9.2*-mediated T1D control.

We have monitored cohorts of (NOD X ICR)F1 and (NOD X ICR)F2 females for diabetes development. None of the (NOD X ICR)F1 (n = 10) and (NOD X ICR)F2 (n = 49) females developed T1D at 30 weeks of age when 97% of our NOD females had become diabetic (n = 34) (data not shown). Since NOD and ICR share the $H2^{g7}$ haplotype, these results indicate that ICR-derived non-MHC diabetes resistance genes dominantly suppress T1D. NOD mice have been outcrossed to a T1D resistant NON stock congenic for the $H2^{g7}$ MHC haplotype to map T1D susceptibility loci [45]. Both NOD and NON mice, as well as the ICR strain used in the current study are derived from the Ha/ICR outbred stock [38]. We also showed previously that NON and ICR mice possessed comparable levels of thymic and splenic iNKT-cells [11]. Taken together, this suggests that enhanced development of iNKT-cells in NON and ICR strains, compared to the NOD mouse, is under the control of at least a subset of the same genetic variants. Therefore, we were particularly interested in determining if the iNKT-cell QTL identified here overlap with previously mapped *Idd* regions in the (NON.$H2^{g7}$ X NOD)F2 cross and the (NON.$H2^{g7}$ X NOD) X NOD first backcross. In this comparison, the *Idd6* complex (Chr 6), *Idd14* (Chr 13), and *Idd15* (Chr 5) mapped for thymic and/or splenic iNKT-cell frequencies in the current study were also found in the (NON.$H2^{g7}$ X NOD)F2 cross to regulate T1D onset [45]. Furthermore, the *Idd9* region on Chr 4 observed to modulate the ratio of splenic CD4/DN iNKT-cells was also identified as a T1D modulating locus in the same (NON.$H2^{g7}$ X NOD)F2 cross [45]. In addition to the co-localization of these iNKT-cell QTL with the *Idd* regions revealed in the (NON.$H2^{g7}$ X NOD)F2 cross, there is also a directional association of alleles that promote T1D resistance and higher frequencies of iNKT-cells or the CD4/DN ratio. The NOD alleles at *Idd9*, *Idd14*, and *Idd15* conferred T1D susceptibility and decreased the frequency and the CD4/DN ratio of iNKT-cells respectively in the previous (NON.$H2^{g7}$ X NOD)F2 and the current (NOD X ICR)F2 crosses [45]. On the other hand, the NOD allele(s) at the *Idd6* complex region promoted T1D resistance in the previous (NON.$H2^{g7}$ X NOD)F2 cross and elevated iNKT-cells in the current study [45]. Collectively, the results suggest that some of these NON-derived T1D resistance or susceptibility loci regulate T1D progression through modulating the iNKT-cell compartment.

Our mapping study also revealed one significant QTL on Chr 12 co-localized with a syntenic human T1D locus. The Chr 12 QTL region has not been identified previously to regulate T1D in NOD mice, but this does not exclude the possibility that a NOD-derived gene(s) within this locus contributes to diabetes development. Overlapping but distinct *Idd*

loci were identified when NOD mice were outcrossed to other diabetes resistant strains [46]. This is because the ability to map these *Idd* loci depends on the presence of genetic polymorphisms between NOD and other parental strains. In the future, we will determine if the ICR-derived Chr 12 region identified here to increase the iNKT-cell frequency also suppresses T1D development in NOD mice. In summary, we have identified several novel loci that regulate iNKT-cell development, a subset of which overlap with previously known mouse *Idd* and syntenic human T1D regions. Although it remains to be determined if the same genes regulate both iNKT-cells and T1D in the overlapping loci identified here, our results provide additional information to facilitate the process of prioritizing regions for future T1D genetic studies.

Materials and Methods

Mice

NOD/ShiLtDvs (hereafter NOD) mice were originally obtained from Dr. D. Serreze's colony at The Jackson Laboratory (TJL) and subsequently maintained at the Medical College of Wisconsin (MCW) by brother-sister mating. ICR/HaJ (hereafter ICR) mice were purchased from TJL (stock number: 009122) and maintained by brother-sister mating at the MCW. NOD females were outcrossed to ICR males to generate F1 animals followed by intercrossing to produce a cohort of F2 progeny. A total of 209 F2 males (7 weeks old) were analyzed for iNKT-cells. Previous studies showed sex difference in the frequency of thymic iNKT-cells [26]. Based on this reason and a potential indirect effect of diabetes development on iNKT-cell homeostasis in females, only male mice were analyzed. All animal protocols were approved by the MCW Institutional Animal Care and Use Committees.

Flow cytometry

Red blood cell depleted single cell suspensions were prepared from the thymus and the spleen. Cells were Fc-blocked at room temperature with anti-CD16/CD32 (clone 2.4G2, BioXCell) for 10 min followed by an antibody cocktail containing CD1d/α-galactosylceramide analog (PBS-57) loaded tetramers, anti-CD4 (clone RM4-5), and anti-TCR_β (clone H57-597) for 30 min at 4°C. CD1d tetramers were provided by the NIH tetramer core facility. Fluorochrome conjugated anti-CD4 and TCR_β antibodies were purchased from BD Bioscience. Stained cells were washed, run on a FACSCalibur flow cytometer (Becton Dickinson), and analyzed using the FlowJo software (Tree Star). Dead cells were excluded by propidium iodide staining.

Genotyping

Tail genomic DNA was purified by the Wizard Genomic DNA Purification kit (Promega). Purified tail DNA samples of all 209 F2 mice were sent to GeneSeek Illumina Genotyping Services (http://www.neogen.com/GeneSeek/SNP_Illumina.html) and genotyped with the Mouse Universal Genotyping Array (MUGA) as previously described [47]. This platform analyzes 7,851 single nucleotide polymorphism (SNP) markers throughout the mouse genome with an average spacing of 325 Kb. NOD, ICR and (NOD x ICR)F1 DNA samples were also included for quality control purposes. Genotypes on these control samples were used to filter out non-informative markers as well as markers with inconsistent genotypes

between parental strains and the F1 sample. A total of 1,624 markers passed the filtering and were used in the QTL mapping analysis. Genetic map positions of these markers (cM) were updated to the new mouse genetic map using the web tool mouse map converter at http://cgd.jax.org [48]. The new map resolves inconsistencies between the physical and genetic maps.

Quantitative trait loci (QTL) analysis

The distributions of measured iNKT-cell phenotypes were skewed so all traits were log-transformed before analysis. A three-stage QTL mapping approach was performed on each of the iNKT-cell traits using R/qtl v1.25-15 (http://www.rqtl.org/) [49] as described [50, 51]. Briefly, the first stage is a single-locus genome scan to identify single loci associated with thymic and splenic iNKT-cell traits (main effect QTL). The respective genome-wide adjusted thresholds for significant ($p < 0.01$) and suggestive ($p < 0.1$) LOD scores were based on 10,000 permutations of the observed data. QTL confidence intervals (CIs) were determined by the posterior probability as previously described [50]. In stage 2 of the analysis, simultaneous pair-wise scans to detect additive and epistatic effects were performed. The third stage was to collect QTL detected at previous 2 stages to construct a multiple-QTL model to determine the combined effects of all QTL detected on the traits. We refine the multiple-QTL model using a backward elimination approach. QTL may be removed if they failed to achieve a stringent significance level ($p < 0.001$) after the effects of other QTL have been taken into consideration. To account for the effects of the thymic output on splenic iNKT-cells, we repeated the QTL analysis of splenic iNKT-cells with their thymic counterpart as an additive covariate. This analysis allowed us to separate the direct effect of a QTL on the splenic iNKT cells from the indirect effects contributed by the thymus.

Supplementary Material

Refer to Web version on PubMed Central for supplementary material.

Acknowledgments

We would like to thank Dr. E. Leiter and Dr. D. Serreze at The Jackson Laboratory for critical reading of the manuscript. We are also grateful to the NIH tetramer core facility for providing us CD1d tetramers. This work was supported by the National Institutes of Health grant DK077443 (to Y.-G. Chen), the American Diabetes Association grant 1-10-BS-26 (to Y.-G. Chen), and the Children's Hospital of Wisconsin Foundation.

References

1. Bendelac A, Savage PB, Teyton L. The biology of NKT cells. Annu Rev Immunol. 2007; 25:297–336. [PubMed: 17150027]
2. Coquet JM, Chakravarti S, Kyparissoudis K, McNab FW, Pitt LA, McKenzie BS, et al. Diverse cytokine production by NKT cell subsets and identification of an IL-17-producing CD4-NK1. 1-NKT cell population. Proc Natl Acad Sci U S A. 2008; 105(32):11287–92. [PubMed: 18685112]
3. Michel ML, Keller AC, Paget C, Fujio M, Trottein F, Savage PB, et al. Identification of an IL-17-producing NK1. 1(neg) iNKT cell population involved in airway neutrophilia. J Exp Med. 2007; 204(5):995–1001. [PubMed: 17470641]
4. Matsuda JL, Mallevaey T, Scott-Browne J, Gapin L. CD1d-restricted iNKT cells, the 'Swiss-Army knife' of the immune system. Curr Opin Immunol. 2008; 20(3):358–68. [PubMed: 18501573]

5. Chan AC, Serwecinska L, Cochrane A, Harrison LC, Godfrey DI, Berzins SP. Immune characterization of an individual with an exceptionally high natural killer T cell frequency and her immediate family. Clin Exp Immunol. 2009; 156(2):238–45. [PubMed: 19250277]
6. Montoya CJ, Pollard D, Martinson J, Kumari K, Wasserfall C, Mulder CB, et al. Characterization of human invariant natural killer T subsets in health and disease using a novel invariant natural killer T cell-clonotypic monoclonal antibody, 6B11. Immunology. 2007; 122(1):1–14. [PubMed: 17662044]
7. Kis J, Engelmann P, Farkas K, Richman G, Eck S, Lolley J, et al. Reduced CD4+ subset and Th1 bias of the human iNKT cells in Type 1 diabetes mellitus. J Leukoc Biol. 2007; 81 (3):654–62. [PubMed: 17151140]
8. Berzins SP, Cochrane AD, Pellicci DG, Smyth MJ, Godfrey DI. Limited correlation between human thymus and blood NKT cell content revealed by an ontogeny study of paired tissue samples. Eur J Immunol. 2005; 35(5):1399–407. [PubMed: 15816002]
9. Lee PT, Putnam A, Benlagha K, Teyton L, Gottlieb PA, Bendelac A. Testing the NKT cell hypothesis of human IDDM pathogenesis. J Clin Invest. 2002; 110(6):793–800. [PubMed: 12235110]
10. Rymarchyk SL, Lowenstein H, Mayette J, Foster SR, Damby DE, Howe IW, et al. Widespread natural variation in murine natural killer T-cell number and function. Immunology. 2008; 125(3): 331–43. [PubMed: 18445005]
11. Chen YG, Tsaih SW, Serreze DV. Genetic control of murine invariant natural killer T-cell development dynamically differs dependent on the examined tissue type. Genes Immun. 2012; 13(2):164–74. [PubMed: 21938016]
12. Berzins SP, Smyth MJ, Baxter AG. Presumed guilty: natural killer T cell defects and human disease. Nat Rev Immunol. 2011; 11(2):131–42. [PubMed: 21267014]
13. Wilson SB, Delovitch TL. Janus-like role of regulatory iNKT cells in autoimmune disease and tumour immunity. Nat Rev Immunol. 2003; 3(3):211–22. [PubMed: 12658269]
14. Naumov YN, Bahjat KS, Gausling R, Abraham R, Exley MA, Koezuka Y, et al. Activation of CD1d-restricted T cells protects NOD mice from developing diabetes by regulating dendritic cell subsets. Proc Natl Acad Sci U S A. 2001; 98(24):13838–43. [PubMed: 11707602]
15. Hong S, Wilson MT, Serizawa I, Wu L, Singh N, Naidenko OV, et al. The natural killer T-cell ligand alpha-galactosylceramide prevents autoimmune diabetes in non-obese diabetic mice. Nat Med. 2001; 7(9):1052–6. [PubMed: 11533710]
16. Sharif S, Arreaza GA, Zucker P, Mi QS, Sondhi J, Naidenko OV, et al. Activation of natural killer T cells by alpha-galactosylceramide treatment prevents the onset and recurrence of autoimmune Type 1 diabetes. Nat Med. 2001; 7(9):1057–62. [PubMed: 11533711]
17. Wang B, Geng YB, Wang CR. CD1-restricted NK T cells protect nonobese diabetic mice from developing diabetes. J Exp Med. 2001; 194(3):313–20. [PubMed: 11489950]
18. Shi FD, Flodstrom M, Balasa B, Kim SH, Van Gunst K, Strominger JL, et al. Germ line deletion of the CD1 locus exacerbates diabetes in the NOD mouse. Proc Natl Acad Sci U S A. 2001; 98(12): 6777–82. [PubMed: 11390999]
19. Lehuen A, Lantz O, Beaudoin L, Laloux V, Carnaud C, Bendelac A, et al. Overexpression of natural killer T cells protects Valpha14- Jalpha281 transgenic nonobese diabetic mice against diabetes. J Exp Med. 1998; 188(10):1831–9. [PubMed: 9815260]
20. Hammond KJ, Poulton LD, Palmisano LJ, Silveira PA, Godfrey DI, Baxter AG. alpha/beta-T cell receptor (TCR)+CD4-CD8- (NKT) thymocytes prevent insulin-dependent diabetes mellitus in nonobese diabetic (NOD)/Lt mice by the influence of interleukin (IL)-4 and/or IL-10. J Exp Med. 1998; 187(7):1047–56. [PubMed: 9529321]
21. Zekavat G, Mozaffari R, Arias VJ, Rostami SY, Badkerhanian A, Tenner AJ, et al. A novel CD93 polymorphism in non-obese diabetic (NOD) and NZB/W F1 mice is linked to a CD4+ iNKT cell deficient state. Immunogenetics. 2010; 62(6):397–407. [PubMed: 20387063]
22. Ueno A, Wang J, Cheng L, Im JS, Shi Y, Porcelli SA, et al. Enhanced early expansion and maturation of semi-invariant NK T cells inhibited autoimmune pathogenesis in congenic nonobese diabetic mice. J Immunol. 2008; 181(10):6789–96. [PubMed: 18981096]

23. Fletcher JM, Jordan MA, Snelgrove SL, Slattery RM, Dufour FD, Kyparissoudis K, et al. Congenic analysis of the NKT cell control gene Nkt2 implicates the peroxisomal protein Pxmp4. J Immunol. 2008; 181(5):3400–12. [PubMed: 18714012]
24. Chen YG, Driver JP, Silveira PA, Serreze DV. Subcongenic analysis of genetic basis for impaired development of invariant NKT cells in NOD mice. Immunogenetics. 2007; 59 (9):705–12. [PubMed: 17619875]
25. Matsuki N, Stanic AK, Embers ME, Van Kaer L, Morel L, Joyce S. Genetic dissection of V alpha 14J alpha 18 natural T cell number and function in autoimmune-prone mice. J Immunol. 2003; 170(11):5429–37. [PubMed: 12759418]
26. Esteban LM, Tsoutsman T, Jordan MA, Roach D, Poulton LD, Brooks A, et al. Genetic control of NKT cell numbers maps to major diabetes and lupus loci. J Immunol. 2003; 171(6):2873–8. [PubMed: 12960309]
27. Jordan MA, Fletcher JM, Jose R, Chowdhury S, Gerlach N, Allison J, et al. Role of SLAM in NKT Cell Development Revealed by Transgenic Complementation in NOD Mice. J Immunol. 2011; 186(7):3953–65. [PubMed: 21357537]
28. Jordan MA, Fletcher JM, Pellicci D, Baxter AG. Slamf1, the NKT cell control gene Nkt1. J Immunol. 2007; 178(3):1618–27. [PubMed: 17237411]
29. Griewank K, Borowski C, Rietdijk S, Wang N, Julien A, Wei DG, et al. Homotypic interactions mediated by Slamf1 and Slamf6 receptors control NKT cell lineage development. Immunity. 2007; 27(5):751–62. [PubMed: 18031695]
30. Kukreja A, Cost G, Marker J, Zhang C, Sun Z, Lin-Su K, et al. Multiple immuno-regulatory defects in type-1 diabetes. J Clin Invest. 2002; 109(1):131–40. [PubMed: 11781358]
31. Wilson SB, Kent SC, Patton KT, Orban T, Jackson RA, Exley M, et al. Extreme Th1 bias of invariant Valpha24JalphaQ T cells in type 1 diabetes. Nature. 1998; 391(6663):177–81. [PubMed: 9428763]
32. Roman-Gonzalez A, Moreno ME, Alfaro JM, Uribe F, Latorre-Sierra G, Rugeles MT, et al. Frequency and function of circulating invariant NKT cells in autoimmune diabetes mellitus and thyroid diseases in Colombian patients. Hum Immunol. 2009; 70(4):262–8. [PubMed: 19480856]
33. Nakamura T, Sonoda KH, Faunce DE, Gumperz J, Yamamura T, Miyake S, et al. CD4+ NKT cells, but not conventional CD4+ T cells, are required to generate efferent CD8+ T regulatory cells following antigen inoculation in an immune-privileged site. J Immunol. 2003; 171(3):1266–71. [PubMed: 12874214]
34. Roelofs-Haarhuis K, Wu X, Gleichmann E. Oral tolerance to nickel requires CD4+ invariant NKT cells for the infectious spread of tolerance and the induction of specific regulatory T cells. J Immunol. 2004; 173(2):1043–50. [PubMed: 15240692]
35. Terabe M, Matsui S, Noben-Trauth N, Chen H, Watson C, Donaldson DD, et al. NKT cell-mediated repression of tumor immunosurveillance by IL-13 and the IL-4R-STAT6 pathway. Nat Immunol. 2000; 1(6):515–20. [PubMed: 11101874]
36. Chen YG, Chen J, Osborne MA, Chapman HD, Besra GS, Porcelli SA, et al. CD38 is required for the peripheral survival of immunotolerogenic CD4+ invariant NK T cells in nonobese diabetic mice. J Immunol. 2006; 177(5):2939–47. [PubMed: 16920929]
37. Simoni Y, Gautron AS, Beaudoin L, Bui LC, Michel ML, Coumoul X, et al. NOD mice contain an elevated frequency of iNKT17 cells that exacerbate diabetes. Eur J Immunol. 2011; 41(12):3574–85. [PubMed: 22002883]
38. Leiter, EA.; Mark, editors. NOD mice and related strains: research applications in diabetes, AIDS, cancer and other diseases. R.G. Lands Company; 1998.
39. Wallace C, Smyth DJ, Maisuria-Armer M, Walker NM, Todd JA, Clayton DG. The imprinted DLK1-MEG3 gene region on chromosome 14q32.2 alters susceptibility to type 1 diabetes. Nat Genet. 2010; 42(1):68–71. [PubMed: 19966805]
40. Serreze DV, Prochazka M, Reifsnyder PC, Bridgett MM, Leiter EH. Use of recombinant congenic and congenic strains of NOD mice to identify a new insulin-dependent diabetes resistance gene. J Exp Med. 1994; 180(4):1553–8. [PubMed: 7931087]

41. Ivakine EA, Fox CJ, Paterson AD, Mortin-Toth SM, Canty A, Walton DS, et al. Sex-specific effect of insulin-dependent diabetes 4 on regulation of diabetes pathogenesis in the nonobese diabetic mouse. J Immunol. 2005; 174(11):7129–40. [PubMed: 15905556]
42. Godfrey DI, Berzins SP. Control points in NKT-cell development. Nat Rev Immunol. 2007; 7(7): 505–18. [PubMed: 17589542]
43. Godfrey DI, Stankovic S, Baxter AG. Raising the NKT cell family. Nat Immunol. 2010; 11 (3): 197–206. [PubMed: 20139988]
44. Ziegler AG, Nepom GT. Prediction and pathogenesis in type 1 diabetes. Immunity. 2010; 32 (4): 468–78. [PubMed: 20412757]
45. McAleer MA, Reifsnyder P, Palmer SM, Prochazka M, Love JM, Copeman JB, et al. Crosses of NOD mice with the related NON strain. A polygenic model for IDDM Diabetes. 1995; 44(10): 1186–95. [PubMed: 7556956]
46. Driver JP, Serreze DV, Chen YG. Mouse models for the study of autoimmune type 1 diabetes: a NOD to similarities and differences to human disease. Semin Immunopathol. 2011; 33(1):67–87. [PubMed: 20424843]
47. The genome architecture of the Collaborative Cross mouse genetic reference population. Genetics. 2012; 190(2):389–401. [PubMed: 22345608]
48. Cox A, Ackert-Bicknell CL, Dumont BL, Ding Y, Bell JT, Brockmann GA, et al. A new standard genetic map for the laboratory mouse. Genetics. 2009; 182(4):1335–44. [PubMed: 19535546]
49. Broman KW, Wu H, Sen S, Churchill GA. R/qtl: QTL mapping in experimental crosses. Bioinformatics. 2003; 19(7):889–90. [PubMed: 12724300]
50. Sen S, Churchill GA. A statistical framework for quantitative trait mapping. Genetics. 2001; 159(1):371–87. [PubMed: 11560912]
51. Wergedal JE, Ackert-Bicknell CL, Tsaih SW, Sheng MH, Li R, Mohan S, et al. Femur mechanical properties in the F2 progeny of an NZB/B1NJ x RF/J cross are regulated predominantly by genetic loci that regulate bone geometry. J Bone Miner Res. 2006; 21 (8):1256–66. [PubMed: 16869724]

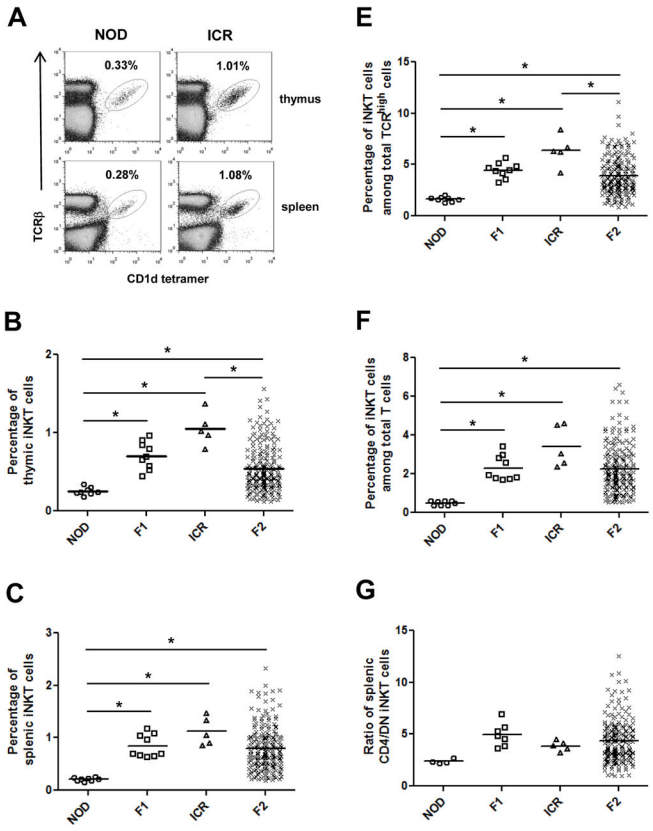

Figure 1. Frequencies and subsets of iNKT-cells in NOD, ICR, (NOD X ICR)F1, and (NOD X ICR)F2 mice

Single cell suspension was prepared from the thymus and the spleen of each mouse (all were 7-week-old males). Cells were stained with anti-TCR_{β}, anti-CD4, and CD1d tetramers. iNKT-cells were identified by co-staining of anti-TCR_{β} and CD1d tetramers. (A) Representative plots of FACS analysis. The frequencies of thymic and splenic iNKT-cells in NOD and ICR mice are shown in the plots. (B) The percentages of thymic iNKT-cells among total thymocytes in NOD, ICR, (NOD X ICR)F1, and (NOD X ICR)F2 mice. (C) The percentages of splenic iNKT-cells among total splenocytes in NOD, ICR, (NOD X ICR)F1, and (NOD X ICR)F2 mice. (D) The percentages of thymic iNKT-cells among TCR^{high} cells in NOD, ICR, (NOD X ICR)F1, and (NOD X ICR)F2 mice. (E) The percentages of splenic iNKT-cells among TCR^{+} cells in NOD, ICR, (NOD X ICR)F1, and (NOD X ICR)F2 mice. (F) The ratios of $CD4^{+}$ and DN iNKT-cells in the spleen of NOD, ICR, (NOD X ICR)F1, and (NOD X ICR)F2 mice. Subsets (CD4 or DN) of iNKT-cells were identified based on the expression of CD4. In panels B-F, each symbol represents one mouse. The horizontal bars indicate the means. * $p < 0.05$ (one way ANOVA followed by Tukey-Kramer post test to compare all possible pairs).

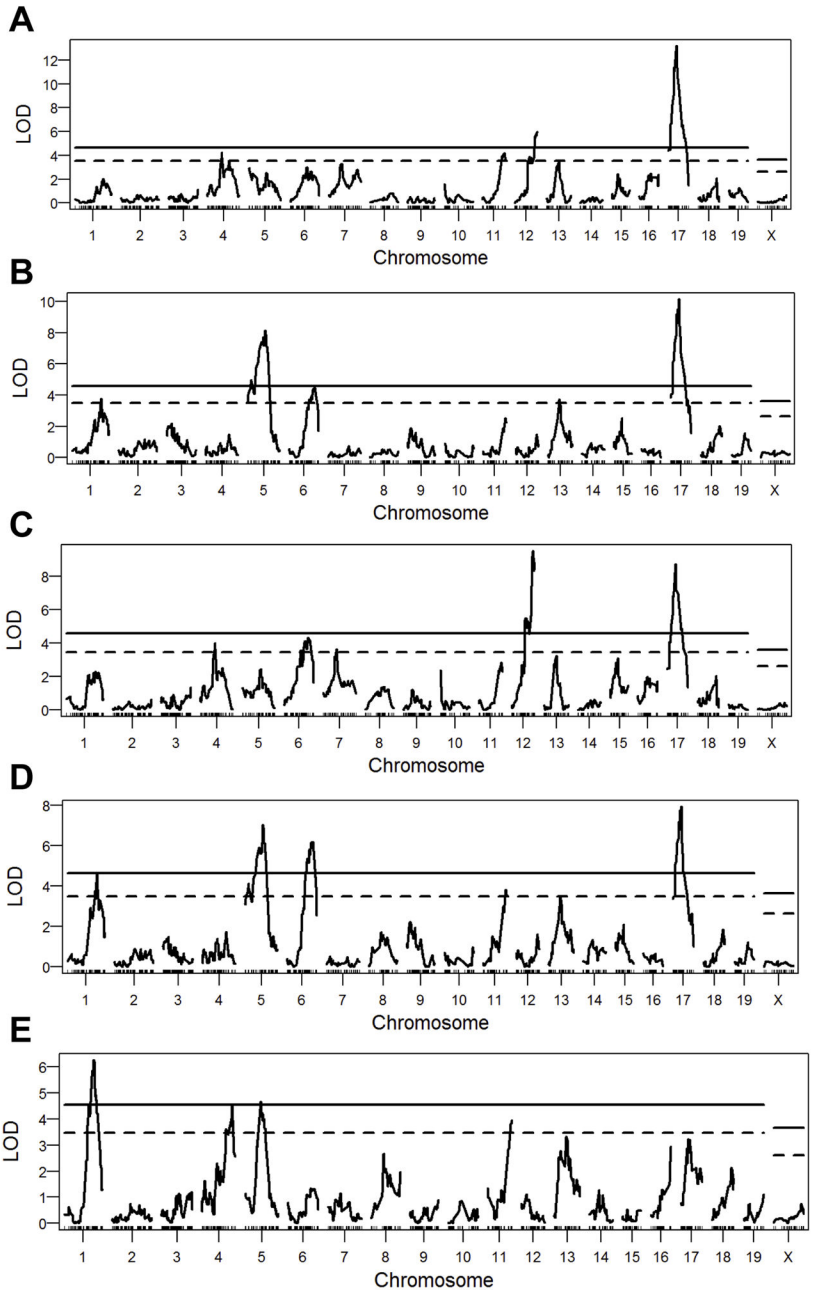

Figure 2. Genome-wide scans for main effect iNKT-cell QTL

(A) The LOD score plot of thymic iNKT-cell frequency among total thymocytes. (B) The LOD score plot of splenic iNKT-cell frequency among total splenocytes. (C) The LOD score plot of thymic iNKT-cell frequency among TCR^{high} cells. (D) The LOD score plot of splenic iNKT-cell frequency among TCR^{+} cells. (E) The LOD score plot of the ratio of splenic $CD4^{+}$ and DN iNKT-cells. The solid and dashed lines respectively represent the genome-wide adjusted significant ($p < 0.01$) and suggestive ($p < 0.1$) LOD score thresholds.

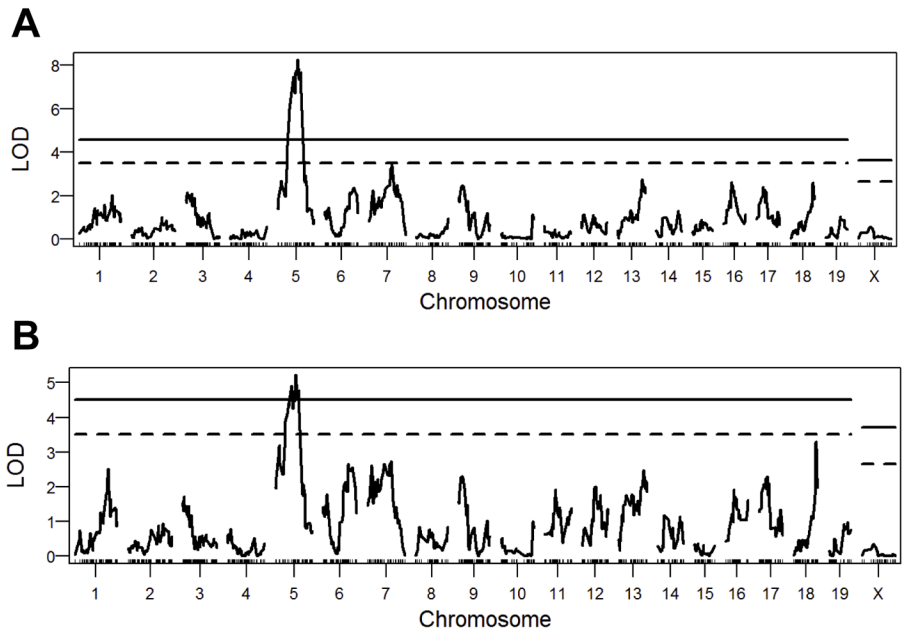

Figure 3. Identification of spleen-specific iNKT-cell QTL

Genome-wide scans for main effect splenic iNKT-cell QTL were conducted with the frequency of thymic iNKT-cells from the same mouse as a covariant (see Materials and Methods). (A) The LOD score plot of thymus-conditioned splenic iNKT-cell frequency among total splenocytes. (B) The LOD score plot of thymus-conditioned splenic iNKT-cell frequency among TCR^+ cells. The solid and dashed lines respectively represent the genome-wide adjusted significant ($p < 0.01$) and suggestive ($p < 0.1$) LOD score thresholds.

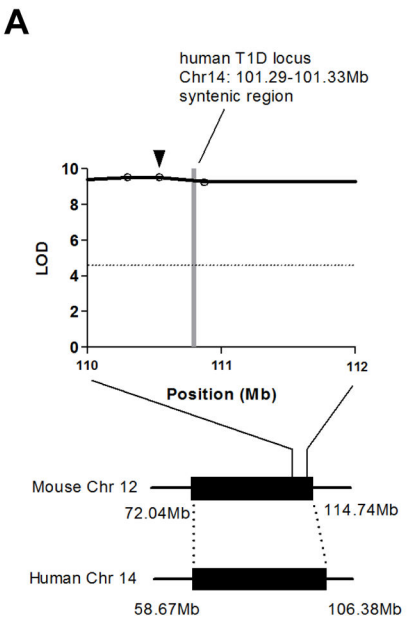

B

Position (Mb)	LOD score
▶ 106.11	5.64
108.94	9.19
109.31	9.12
110.30	***9.53***
110.53	***9.53***
110.87	***9.28***
112.02	9.28
112.25	9.28
113.41	9.11
113.45	9.11
113.75	9.11
114.04	9.11
114.81	8.32
115.89	8.56
116.93	8.56
117.87	8.60
118.51	8.84
119.43	8.46
119.95	8.46
→ 120.58	8.46

Figure 4. Comparison of the mouse Chr 12 iNKT-cell QTL and a syntenic human T1D region

(A) The LOD score plot of the thymic iNKT-cell QTL (percentage of TCR^{high} cells) on Chr 12 in relation to a human syntenic T1D region on Chr 14. The dotted lines indicate the genome-wide adjusted significant ($p < 0.01$) LOD score threshold. The gray bar represents the syntenic human T1D region based on information obtained from T1Dbase (www.t1dbase.org). The circles depict the locations of informative SNP markers that were typed for the QTL analysis. The arrowhead indicates the location of the peak LOD score in the region. The extended orthologous regions (filled black boxes) between mouse Chr 12 (72.04Mb to 114.74Mb) and human Chr 14 (58.67Mb to 106.38Mb) are also shown at the bottom of the panel. The extended mouse and human orthologous regions were obtained from Ensembl genome browser based on mouse NCBI Build 37 (www.ensembl.org). The length of the chromosome is not drawn to scale. (B) The LOD scores of informative SNP markers, shown in positions, adjacent to the linkage peak illustrated in panel A. The arrow head indicates the first marker that shows a drop of more than 1 LOD from the peak. The arrow denotes the most distal informative marker on the chromosome on the SNP typing array. Bold and italic fonts indicate the markers that are displayed in panel A.

Table 1

Summary of genome scans for significant main effect thymic iNKT-cell QTL

Chromosome	Peak location[1] (95% CI)[2]	% iNKT of total cells LOD score (*p* value)[3]	High allele	% iNKT of TCR^{high} LOD score (*p* value)	High allele
12	110.30 (108.94–118.51)			9.53 (< 10^{-9})	ICR
	118.51 (108.94–120.58)	5.97 (0.0002)	ICR		
17	50.43 (45.76–50.43)	13.21 (< 10^{-9})	NOD	8.73 (< 10^{-9})	NOD

[1] Megabase (Mb) positions from NCBI Build 37.

[2] 95% confidence interval. If the peak location is the same for both traits, only the interval for the highest LOD score is shown.

[3] Permutation adjusted *p* value.

Table 2

Summary of genome scans for significant main effect splenic iNKT-cell QTL

Chromosome	Peak location[1] (95% CI)[2]	% iNKT of total cells LOD score (*p* value)[3]	High allele	% iNKT of TCR$^+$ LOD score (*p* value)	High allele	CD4/DN ratio LOD score (*p* value)	High allele	Overlapping *Idd*
1	171.62 (166.74–174.57)					6.27 (0.0002)	ICR	
	172.96 (140.86–185.40)			4.66 (0.0096)	ICR			
4	148.85 (130.98–148.85)					4.57 (0.0096)	ICR	*Idd9.2*
5	79.45 (72.62–109.49)					4.68 (0.0076)	ICR	
	100.54 (64.46–109.49)	8.16 (< 10^{-9})	ICR					
	101.11 (64.46–113.63)			7.04 (< 10^{-9})	ICR			
6	138.66 (115.59–138.67)			6.19 (0.0002)	NOD			*Idd6.2*
17	50.43 (36.08–50.43)	10.17 (< 10^{-9})	NOD	7.95 (< 10^{-9})	NOD			

[1] Megabase (Mb) positions from NCBI Build 37.

[2] 95% confidence interval. If the peak location is the same for multiple traits, only the interval for the highest LOD score is shown.

[3] Permutation adjusted *p* value.

Table 3

Summary of multiple regression analyses of thymic iNKT-cell QTL

Chromosome	Peak location[1]	% iNKT of total cells (LOD score)	% iNKT of TCR^{high} (LOD score)	*Overlapping Idd*
4	89.50	7.54	8.96	
5	9.30	5.85		*Idd15*
6	133.92		6.64	*Idd6.2 and Idd19* regions
11	97.16	5.07		
12	110.30		16.80	
	118.51	9.62		
13	70.73	8.17	4.78	*Idd14*
	119.54	4.60		*Idd14*
15	59.69		6.14	
17	50.43	19.95	16.86	

[1] Megabase (Mb) positions from NCBI Build 37.

Table 4

Summary of multiple regression analyses of splenic iNKT-cell QTL

Chromosome	Peak location[1]	% iNKT of total cells (LOD score)	% iNKT of TCR$^+$ (LOD score)	CD4/DN ratio	Overlapping *Idd*
1	171.62			8.24	
	172.96	5.78	7.43		
4	148.85			3.85	*Idd9.2*
5	24.43	3.96			
	79.45			5.01	
	101.11	7.25	7.40		
6	138.66	3.39	6.54		*Idd6.2*
8	74.44			4.05	
11	97.16		5.24		
	99.91			4.69	
13	62.03	6.71	6.25	5.58	*Idd14*
16	92.13			5.37	
17	50.43	13.01	10.38	4.58	

[1] Megabase (Mb) positions from NCBI Build 37.